Molecular diversity and associated phenotypic spectrum of germline CBL mutations

Martinelli, Simone ; Stellacci, Emilia ; Pannone, Luca ; D'Agostino, Daniela ; Consoli, Federica ; Lissewski, Christina ; Silvano, Marianna ; Cencelli, Giulia ; Lepri, Francesca ; Maitz, Silvia ; Pauli, Silke ; Rauch, Anita ; Zampino, Giuseppe ; Selicorni, Angelo ; Melançon, Serge ; Digilio, Maria C ; Gelb, Bruce D ; De Luca, Alessandro ; Dallapiccola, Bruno ; Zenker, Martin ; Tartaglia, Marco

Abstract: Noonan syndrome (NS) is a relatively common developmental disorder with a pleomorphic phenotype. Mutations causing NS alter genes encoding proteins involved in the RAS-MAPK pathway. We and others identified Casitas B-lineage lymphoma proto-oncogene (CBL), which encodes an E3-ubiquitin ligase acting as a tumor suppressor in myeloid malignancies, as a disease gene underlying a condition clinically related to NS. Here, we further explored the spectrum of germline CBL mutations and their associated phenotype. CBL mutation scanning performed on 349 affected subjects with features overlapping NS and no mutation in NS genes allowed the identification of five different variants with pathological significance. Among them, two splice-site changes, one in-frame deletion, and one missense mutation affected the RING domain and/or the adjacent linker region, overlapping cancer-associated defects. A novel nonsense mutation generating a v-Cbl-like protein able to enhance signal flow through RAS was also identified. Genotype-phenotype correlation analysis performed on available records indicated that germline CBL mutations cause a variable phenotype characterized by a relatively high frequency of neurological features, predisposition to juvenile myelomonocytic leukemia, and low prevalence of cardiac defects, reduced growth, and cryptorchidism. Finally, we excluded a major contribution of two additional members of the CBL family, CBLB and CBLC, to NS and related disorders.

DOI: https://doi.org/10.1002/humu.22809

RESEARCH ARTICLE

Human Mutation

OFFICIAL JOURNAL HGVS HUMAN GENOME VARIATION SOCIETY www.hgvs.org

Molecular Diversity and Associated Phenotypic Spectrum of Germline *CBL* Mutations

Simone Martinelli,[1]* Emilia Stellacci,[1] Luca Pannone,[1,2] Daniela D'Agostino,[3] Federica Consoli,[2,4] Christina Lissewski,[5] Marianna Silvano,[1]† Giulia Cencelli,[1] Francesca Lepri,[6] Silvia Maitz,[7] Silke Pauli,[8] Anita Rauch,[9] Giuseppe Zampino,[10] Angelo Selicorni,[7] Serge Melançon,[3] Maria C. Digilio,[6] Bruce D. Gelb,[11] Alessandro De Luca,[4] Bruno Dallapiccola,[6] Martin Zenker,[5] and Marco Tartaglia[1]‡

[1] *Dipartimento di Ematologia, Oncologia e Medicina Molecolare, Istituto Superiore di Sanità, Rome, Italy;* [2] *Dipartimento di Medicina Sperimentale, Sapienza Università di Roma, Rome, Italy;* [3] *Department of Medical Genetics, McGill University Health Centre, Montreal Children's Hospital, Montreal, Quebec, Canada;* [4] *Laboratorio Mendel, Istituto di Ricovero e Cura a Carattere Scientifico-Casa Sollievo della Sofferenza, Rome, Italy;* [5] *Institute of Human Genetics, University Hospital of Magdeburg, Otto-von-Guericke-University, Magdeburg, Germany;* [6] *Ospedale Pediatrico "Bambino Gesù", Rome, Italy;* [7] *Dipartimento di Pediatria, Genetica Clinica, Ospedale S. Gerardo, Università di Milano-Bicocca, Monza, Italy;* [8] *Institute of Human Genetics, University of Göttingen, Göttingen, Germany;* [9] *Institute of Medical Genetics, University of Zurich, Schlieren-Zurich, Switzerland;* [10] *Istituto di Clinica Pediatrica, Università Cattolica del Sacro Cuore, Rome, Italy;* [11] *Mindich Child Health and Development Institute and Departments of Pediatrics and Genetics and Genomic Sciences, Icahn School of Medicine at Mount Sinai, New York*

Communicated by Ming Qi

Received 15 January 2015; accepted revised manuscript 30 April 2015.
Published online 8 May 2015 in Wiley Online Library (www.wiley.com/humanmutation). DOI: 10.1002/humu.22809

ABSTRACT: Noonan syndrome (NS) is a relatively common developmental disorder with a pleomorphic phenotype. Mutations causing NS alter genes encoding proteins involved in the RAS-MAPK pathway. We and others identified Casitas B-lineage lymphoma proto-oncogene (*CBL*), which encodes an E3-ubiquitin ligase acting as a tumor suppressor in myeloid malignancies, as a disease gene underlying a condition clinically related to NS. Here, we further explored the spectrum of germline *CBL* mutations and their associated phenotype. *CBL* mutation scanning performed on 349 affected subjects with features overlapping NS and no mutation in NS genes allowed the identification of five different variants with pathological significance. Among them, two splice-site changes, one in-frame deletion, and one missense mutation affected the RING domain and/or the adjacent linker region, overlapping cancer-associated defects. A novel nonsense mutation generating a *v*-Cbl-like protein able to enhance signal flow through RAS was also identified. Genotype–phenotype correlation analysis performed on available records indicated that germline *CBL* mutations cause a variable phenotype characterized by a relatively high frequency of neurological features, predisposition to juvenile myelomonocytic leukemia, and low prevalence of cardiac defects, reduced growth, and cryptorchidism. Finally, we excluded a major contribution of two additional members of the CBL family, *CBLB* and *CBLC*, to NS and related disorders.

Hum Mutat 36:787–796, 2015. © 2015 Wiley Periodicals, Inc.

KEY WORDS: *CBL* mutation-associated syndrome; Noonan syndrome; RAS-MAPK; genotype–phenotype correlations

Introduction

Noonan syndrome (NS; MIM #163950) is an autosomal-dominant, relatively common, and clinically variable condition with an estimated prevalence of one in 1,000–2,500 live births [Mendez and Opitz, 1985]. It is characterized by postnatal reduced growth, facial dysmorphism, and congenital heart defects (CHDs) [Allanson, 2007; van der Burgt, 2007; Roberts et al., 2013]. Although the facial dysmorphia changes with age, the most recurrent features consist of a broad forehead, hypertelorism, downslanting palpebral fissures, ptosis, epicanthal folds, and low-set, posteriorly rotated ears with thick helices. Apart from Down syndrome, NS is the most common syndromic cause of CHDs [Burch et al., 1993; Marino et al., 1999; Shaw et al., 2007]. Cardiac involvement is present in up to 80% of affected individuals, with pulmonary valve stenosis, hypertrophic cardiomyopathy (HCM), and septal defects occurring most commonly. Other associated features include chest and spine defects, ectodermal anomalies, webbed/short neck, variable cognitive deficits, cryptorchidism, delayed puberty, lymphatic dysplasia, and a wide spectrum of hematologic abnormalities, including transient monocytosis, coagulation defects, and, rarely, certain malignancies of infancy and childhood [Tartaglia et al., 2003; Jongmans et al., 2011; Kratz et al., 2011; Aoki and Matsubara, 2013].

Additional Supporting Information may be found in the online version of this article.

†Marianna Silvano's present address is Dipartimento di Medicina Molecolare, Sapienza Università di Roma, Rome, Italy.

‡Correspondence to: Marco Tartaglia, Department of Hematology, Oncology and Molecular Medicine, Istituto Superiore di Sanità, Viale Regina Elena, 299, Rome 00161, Italy. E-mail: marco.tartaglia@iss.it

*Correspondence to: Simone Martinelli, Department of Hematology, Oncology and Molecular Medicine, Istituto Superiore di Sanità, Viale Regina Elena, 299, Rome 00161, Italy. E-mail: simone.martinelli@iss.it

Contract grant sponsors: Telethon-Italy (GGP13107); AIRC (IG 13360); Italian Ministry of Health (RF-2010-2310935 and RC-2014, and RF-2011-02349938); German Research Foundation (DFG; ZE 524/9-1).

NS is genetically heterogeneous. Extensive studies performed in the last decade demonstrated that all the genes implicated in NS and related phenotypes encode proteins with a role in the RAS signaling, with disease-causing mutations generally enhancing signal flow through the MAPK cascade but also perturbing signal flow through other RAS-mediated pathways [Tartaglia et al., 2011]. Germline missense, gain-of-function mutations in *PTPN11*, which encodes SHP2, a cytoplasmic protein tyrosine phosphatase that functions as a positive regulator of RAS signaling [Neel et al., 2003], occur in approximately 50% of NS subjects [Tartaglia et al., 2001, 2002]. Activating mutations in seven additional genes coding for transducers or modulatory proteins participating in this pathway (i.e., *SOS1*, *KRAS*, *NRAS*, *RIT1*, *RAF1*, *BRAF*, and *MAP2K1*) account for an additional one-fourth of cases [Tartaglia et al., 2011; Aoki et al., 2013]. Remarkably, mutations in the same genes and other functionally related loci have been reported to underlie a group of clinically related conditions, which have been collectively named "RASopathies" [Aoki et al., 2008; Tartaglia and Gelb, 2010; Rauen, 2013; Flex et al., 2014].

We and others recently reported that germline mutations in the Casitas B-lineage lymphoma proto-oncogene (*CBL*; MIM #165360) cause a previously unrecognized condition that resembles NS phenotypically and predispose to juvenile myelomonocytic leukemia (JMML; MIM #607785) (*CBL* mutation-associated syndrome, hereinafter) [Martinelli et al., 2010; Niemeyer et al., 2010; Pérez et al., 2010]. *CBL* encodes a RING finger E3 ubiquitin ligase that negatively regulates intracellular signaling, targeting receptor tyrosine kinases (RTKs) for internalization and recycling/degradation [Swaminathan and Tsygankov, 2006; Dikic and Schmidt, 2007]. On the other hand, CBL positively modulates signal traffic through its adaptor function. Somatically acquired *CBL* mutations occur with variable prevalence in myeloid malignancies, including JMML, and are generally observed as homozygous lesions due to loss of the wild-type allele by acquired isodisomy of the 11q23 chromosomal region [Kales et al., 2010]. Collected data indicate that disease-associated mutations are predominantly splice site or missense changes affecting exons 8 and 9, which encode the RING finger domain and/or the adjacent linker helix region (LHR) connecting this domain to the *N*-terminal tyrosine kinase binding (TKB) domain. In line with studies focused on cancer-associated *CBL* mutations [Sargin et al., 2007; Sanada et al., 2009; Martinelli et al., 2012], functional characterization of a panel of RASopathy-causing mutants documented that lesions act in a dominant-negative manner, affecting CBL-mediated receptor ubiquitination, and upregulate signal flow through RAS [Martinelli et al., 2010; Niemeyer et al., 2010; Brand et al., 2014].

CBL mutation-associated syndrome is characterized by phenotypic heterogeneity and variable expressivity. Here, we further investigated the molecular spectrum of germline *CBL* mutations, their impact on protein function, and the clinical features associated with those molecular lesions.

Materials and Methods

Patients

Two cohorts consisting of clinically well-characterized subjects with a clinical diagnosis of NS or features within the RASopathy phenotypic spectrum were included in the study. A first group of patients ($N = 214$) were negative for mutations in genes previously identified to cause NS or a closely related condition (i.e., *PTPN11*, *SOS1*, *KRAS*, *NRAS*, *RIT1*, *RAF1*, *BRAF*, *MAP2K1*, *SHOC2*, and *RRAS*). In the second cohort ($N = 135$), mutations in a subset of disease genes had been excluded (i.e., *PTPN11*, *SOS1*, *RAF1*, *RIT1*, *KRAS*, and *SHOC2*). Nearly all patients of both cohorts were of European ancestry. Subjects were assessed by experienced clinical geneticists and pediatricians. Clinical assessment included physical, anthropometric, neurologic, and cardiac evaluations, as well as accurate examination of craniofacial features, and ophthalmologic, immunologic, ectodermal, and skeletal defects. DNA samples and clinical data were collected under research protocols approved by an institutional review board, and informed consent for genetic analyses was obtained from all patients.

Mutation Analysis

Genomic DNA was isolated from peripheral blood leukocytes and other tissues, according to standard procedures. The entire *CBL* coding sequence (NM_005188.3), as well as the exon/intron boundaries and flanking intronic portions, were scanned for mutations by direct sequencing or DHPLC analysis. Sequencing used the ABI BigDye Terminator Sequencing Kit v.1.1 (Applied Biosystems, Foster City, CA) and an ABI 3700 Capillary Array Sequencer or ABI 3500 Genetic Analyzer (Applied Biosystems). DHPLC screening was performed using the 3100 and/or 3500HT Wave DNA Fragment Analysis System (Transgenomic, Omaha, NE), at column temperatures recommended by the Navigator version 1.5.4.23 software (Transgenomic), as previously described [Martinelli et al., 2010]. Amplimers having abnormal elution profiles were reamplified, purified (Qiagen, Hilden, Germany), and sequenced bidirectionally. Homozygous/hemizygous condition for *CBL* sequence variations was explored by DHPLC analysis using pooled DNAs. Primer pair sequences, and PCR and DHPLC settings are available upon request. Nucleotide numbering of the mutations and exonic disease-unrelated variants reflects cDNA numbering, with 1 corresponding to the A of the ATG translation initiation codon in the reference sequence (NM_005188.3), whereas position of the intronic variants were numbered according to the reference genomic sequence (NG_016808.1).

Mutational screening was also performed on exons 8 and 9 of *CBLB* (NM_170662.3), and exons 7 and 8 of *CBLC* (NM_012116.3). Primer sequences are listed in Supp. Table S1.

When available, parental DNAs were sequenced to establish whether the identified changes in sporadic cases were de novo. Paternity was confirmed using the AmpDESTER ProfilerPlus kit (Applied Biosystems).

Molecular Characterization of Splice-Site Mutations

Total RNA was isolated from circulating leukocytes of case 12520-1 by RNeasy Mini Kit (Qiagen). Reverse transcription was performed using the SuperScriptIII first strand kit (Invitrogen, Carlsbad, CA), following the manufacturer's instructions. RT-PCR was carried out using primers designed to amplify exons 7–9 of *CBL*. Primer sequences are listed in Supp. Table S2. The length of each transcript was determined by cloning purified RT-PCR products in a pCR 2.1 TOPO vector (Qiagen). Individual *Escherichia coli* colonies were amplified, and amplicons were separated by electrophoresis on 2% agarose gel, and sequenced.

RNA was not available for case 827-10. To characterize the effect of the c.1096-1G>T mutation on mRNA processing, we generated wild-type and mutant minigenes, using the exon trapping vector pSPL3 (Life Technologies, Monza, Italy). A genomic DNA fragment encompassing exons 7–9 of *CBL* (Chr11:119147899–119149924)

was amplified by using Intron 6_Fw and Intron 9_Rv primers including the *XhoI* and *NheI* restriction sites, respectively (Supp. Table S2). PCR amplification was performed using the Platinum Taq DNA Polymerase (Invitrogen). The resulting 2,025-bp-length PCR product was purified, digested, and cloned into the pSPL3 vector. The correct sequence of the fragment of interest was confirmed by direct sequencing. COS1 cells were transiently transfected with 4 μg of wild-type or mutant constructs using Fugene 6 (Promega, Milan, Italy). Twenty-four hours after transfection, cells were harvested, total RNA was extracted, and reverse transcription was performed as described above. The resulting cDNAs were amplified using pSPL3-specific primers (SD6 and SA2) and primers to amplify *CBL* exons 7–9. PCR conditions are available upon request.

Functional Studies

The c.705T>A nucleotide substitution was introduced in the *N*-terminally hemagglutinin (HA)-tagged human *CBL* cDNA cloned in the pALTER-MAX vector (Promega) by site-directed mutagenesis (QuikChange Kit; Stratagene, La Jolla, CA). COS1 cells were transiently transfected with wild-type or mutant CBL (4 μg), by using Fugene 6 (Promega). Twenty-four hours post-transfection, cells were serum-starved (16 hr) and then stimulated with EGF (Life Technologies) (100 ng/ml, 30 min). ERK and AKT phosphorylation assays were performed in cells transiently expressing the p.Tyr235*, p.Arg420Gln, and wild-type CBL proteins, as previously described [Martinelli et al., 2010, 2012]. Protein phosphorylation status (pERK1/2 #9106 and pAKT #9271S; Cell Signaling, Danvers, MA) was evaluated basally or after EGF stimulation. ERK1/2 (Cell Signaling, #9102), AKT (Cell Signaling, #9272), CBL (anti-HA antibody; H3663; Sigma–Aldrich, St. Louis, MO) and β-tubulin (T4026; Sigma–Aldrich) expression levels were measured. For time course analysis of CBL stability, 24 hr after transfection, COS1 cells were treated with cycloheximide (Sigma–Aldrich) at 100 μg/ml to prevent protein synthesis, at the indicated times.

Statistical Analysis

P values for genotype–phenotype correlation analyses were calculated using two-tailed Fisher's exact test. The significance threshold was set at $P = 0.05$. Exact confidence intervals of proportions (at 95% level) were calculated based on binomial distribution.

Results

Mutation Analysis and Functional Characterization of Mutations

Three-hundred and forty-nine subjects with clinical diagnosis of NS or having features suggestive of this disorder or within the RASopathy phenotypic spectrum, and without mutations in previously identified NS disease genes were included in the study. Mutation analysis allowed the identification of heterozygosity for a *CBL* mutation in five unrelated individuals (Fig. 1A; Table 1) with a variable phenotype overlapping NS only in part (Supp. Table S3) (NS_EuroNet database, https://nseuronet.com/php/index.php). The c.1111T>C (case 10-0746) and c.1104_1112del (case 13M1230) mutations (p.Tyr371His and p.Glu369_Tyr371del, respectively), as well as the c.1096-4_1096-1delAAAG (case 12520–1) and c.1096-1G>T (case 827-10) splice-site variants were identified in four sporadic cases. Among these, parental DNA was available for three patients, and sequencing of the relevant exon demonstrated the de novo origin of mutations (Table 1). In cases for which DNA from other tissues was available, the *CBL* lesion was documented in oral mucosal epithelial (c.1111T>C) or muscle (c.1096-4_1096-1delAAAG) cells, which excluded a somatic event restricted to hematopoietic cells (Supp. Fig. S1). The c.705T>A substitution in exon 4 was documented in a child (case 05-0562) whose mother and brother showed features within the RASopathy spectrum. DNA specimens from these family members were not available to analyze cosegregation of the mutation with disease. This change, however, was not observed in more than 400 population-matched unaffected individuals scanned by DHPLC analysis and direct sequencing, indicating that this variant does not represent a common disease-unrelated polymorphism occurring in the population. Consistently, this variant had not been reported in public databases (dbSNP138, ExAC, and 1000 genomes). A full list of the disease-unrelated changes, including silent substitutions and intronic variants close to the intron/exon boundaries, is reported in Supp. Table S4. Given the close homology and functional relationship occurring among the three members of the CBL family [Swaminathan and Tsygankov, 2006], the exons of *CBLB* (MIM #604491) and *CBLC* (MIM #608453) encompassing the sequence encoding the RING finger domain and the LHR, which represent the mutational hotspot regions for *CBL* (see below), were analyzed in a subset of 96 subjects within the first cohort. Mutation scanning failed in identifying any disease-causing lesion in these genes, indicating that *CBLB* and *CBLC* are not commonly mutated in RASopathies.

The p.Tyr371His and p.Glu369_Tyr371del mutations involve residues evolutionarily conserved in *CBL* orthologs and paralogs located within the LHR, a region frequently affected by somatic and germline *CBL* lesions (Fig. 1B). Homozygous defects involving Tyr^{371} are the most common event among *CBL* mutation-positive individuals with nonsyndromic JMML [Loh et al., 2009; Muramatsu et al., 2010; Niemeyer et al., 2010]. Leukemia-associated mutations affecting Tyr^{371} were previously shown to abolish RTKs ubiquitination by impairing E3 activity [Levkowitz et al., 1999; Thien et al., 2001; Sanada et al., 2009; Niemeyer et al., 2010], promote cytokine-independent growth and constitutive activation of downstream signaling pathways (i.e., RAS-MAPK and PI3K-AKT) [Niemeyer et al., 2010], and confer oncogenic properties [Kassenbrock and Anderson, 2004; Sanada et al., 2009]. Likewise, p.Glu369_Tyr371del, which had been reported as a somatic event associated with 11q-aUPD in a subject with chronic myelomonocytic leukemia (CMML) [Sanada et al., 2009], is expected to be functionally equivalent to mutations affecting Tyr^{371}.

Both the c.1096-4_1096-1delAAAG and c.1096-1G>T lesions affect the *CBL* splice acceptor site for exon 8. Splice-site mutations affecting introns 7 and 8 account for approximately 10% of *CBL* defects underlying myeloid malignancies [Kales et al., 2010], and are predicted to encode a protein that lacks essential regions of the LHR and/or the RING finger domain. RT-PCR analysis performed on cDNA obtained from total RNA extracted from circulating leukocytes of patient 12520-1 documented aberrant processing of the transcript. Besides the wild-type allele, three smaller products resulting from partial or complete deletion of exon 8 were identified (Fig. 2A and C; Supp. Fig. S2). Interestingly, products 1A and 1B resulted from the use of two alternative splice acceptor sites within exon 8 (c.1118_1119 or c.1166_1167), leading to deletion of the first 8- or 24-hr residues encoded by this exon. The c.1096-1G>T transversion found in case 827-10 had not been previously described, but a different change at the same position (c.1096-1G>C) had been reported [Abbas et al., 2008; Grand et al.,

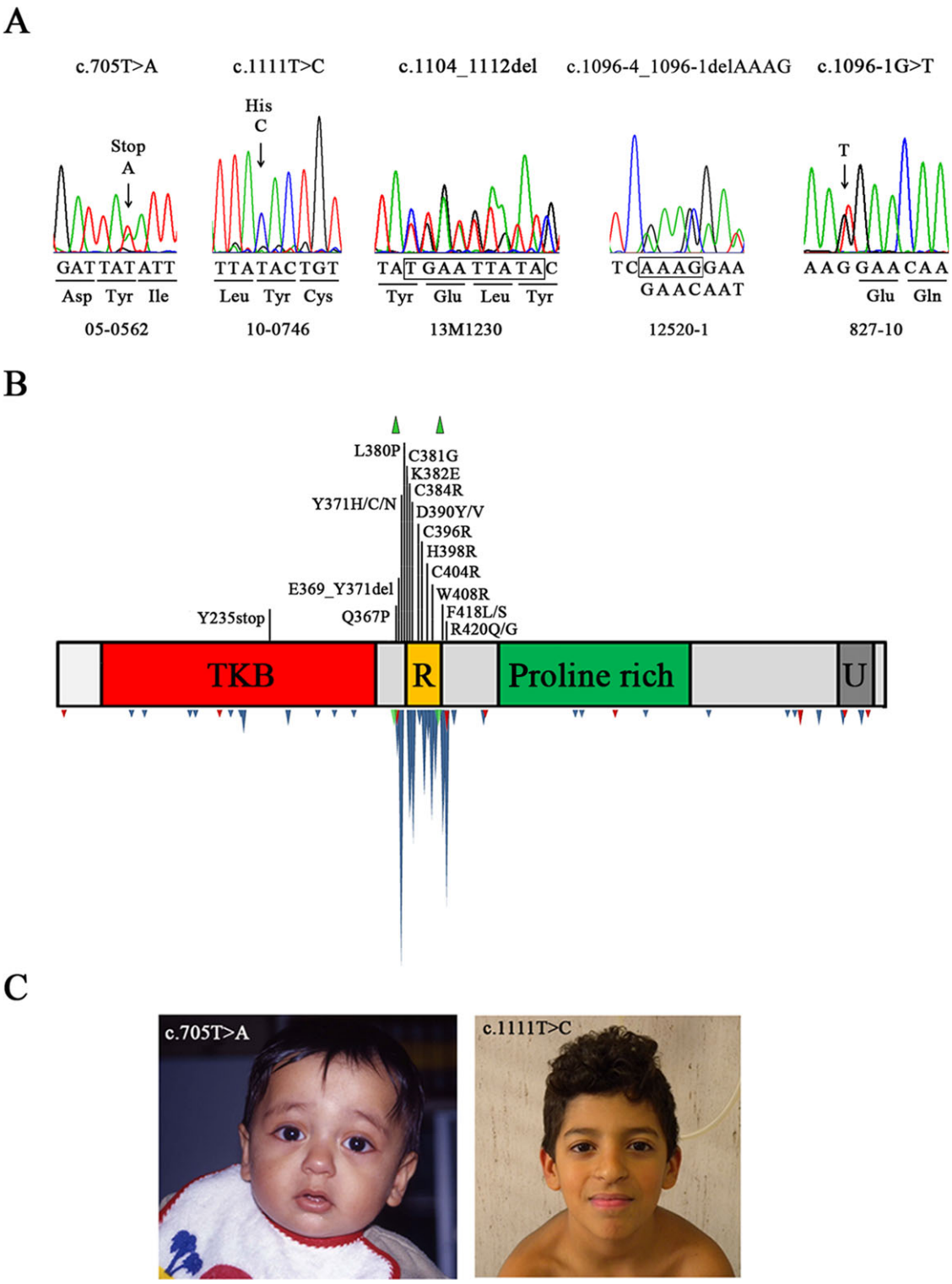

Figure 1. RASopathy-associated germline *CBL* mutations. **A**: Electropherograms showing the heterozygous *CBL* mutations identified in the present study. Nucleotide deletions are shown in open boxes. **B**: Location of germline disease-associated lesions is shown above the CBL domain structure scheme (splice-site changes are shown as green-filled peaks). Forty-four germline *CBL* mutations have been identified to date. Amino acid changes at codons 371 and 367 have been reported in 18 and four unrelated cases, respectively; mutations at codons 390, 418, and 420, and the c.1228-2A>G splice-site change, have been found in two cases; all the other substitutions were described once. The *N*-terminal tyrosine kinase binding domain (TKB) (red), linker helix region (LHR) (light gray), RING-finger domain (RING) (orange), and ubiquitin-associated and leucine zipper domain (UBA/LZ) (dark gray), are shown. The distribution of somatic *CBL* missense (blue-filled peaks), nonsense (red-filled peaks), and splice-site (green-filled peaks) mutations occurring in leukemia is shown below the cartoon (Cosmic database). **C**: Facial features of two affected subjects carrying the c.705T>A (p.Tyr235*) and the c.1111T>C (p.Tyr371His) mutations.

Table 1. List of Previously Reported and Newly Identified Germline *CBL* Gene Mutations

Number of cases	Nucleotide change[a]	Exon	Predicted amino acid change	Domain	Zygosity hematopoietic cells	Zygosity non-hematopoietic cells	Origin of the mutation	Reference
1	c.705T>A	4	p.Tyr235*	TKB	Heterozygous	NA	Familial	Present study
1	c.1096-1G>C	Intron 7	Splice-site change	LHR/RING[b]	Homozygous	Heterozygous	NA	Niemeyer et al. (2010)
1	c.1096-1G>T	Intron 7	Splice-site change	LHR/RING[b]	Heterozygous	NA	De novo	Present study; Bülow et al. (2015)
1	c.1096-1delGG	Intron 7	Splice-site change	LHR/RING[b]	Heterozygous	Heterozygous	De novo	Strullu et al. (2013)
1	c.1096-4_1096-1delAAAG	Intron 7	Splice-site change	LHR/RING[b]	Heterozygous	Heterozygous	NA	Present study
4	c.1100A>C	8	p.Gln367Pro	LHR	Heterozygous	Heterozygous[c]	De novo	Bülow et al. (2015); Martinelli et al. (2010); Hanson et al. (2014)
1	c. 1104_1112del	8	p.Glu369_Tyr371del	LHR	Heterozygous	Heterozygous	De novo	Present study
1	c.1111T>A	8	p.Tyr371Asn	LHR	Homozygous	Heterozygous	NA	Niemeyer et al. (2010)
15	c.1111T>C	8	p.Tyr371His	LHR	Homozygous	Heterozygous	De novo[d]	Niemeyer et al. (2010); Strullu et al. (2013); Pérez et al. (2010); Hyakuna et al. (2015)
1	c.1111T>C	8	p.Tyr371His	LHR	Heterozygous	Heterozygous	De novo	Present study
1	c.1112A>G	8	p.Tyr371Cys	LHR	Homozygous	Heterozygous	Familial	Niemeyer et al. (2010)
1	c.1139T>C	8	p.Leu380Pro	LHR	Homozygous	Heterozygous	NA	Niemeyer et al. (2010)
1	c.1141T>G	8	p.Cys381Gly	LHR	Homozygous	Heterozygous	De novo	Strullu et al. (2013)
1	c.1144A>G	8	p.Lys382Glu	RING	Heterozygous	Heterozygous	Familial	Martinelli et al. (2010)
1	c.1150T>C	8	p.Cys384Arg	RING	Homozygous	Heterozygous	Familial	Niemeyer et al. (2010)
1	c.1168G>T	8	p.Asp390Tyr	RING	Heterozygous	Heterozygous	De novo	Martinelli et al. (2010)
1	c.1169A>T	8	p.Asp390Val	RING	Homozygous	Heterozygous	De novo	Becker et al. (2014)
1	c.1186T>C	8	p.Cys396Arg	RING	Homozygous	Heterozygous	NA	Niemeyer et al. (2010)
1	c.1193A>G	8	p.His398Arg	RING	Homozygous	Heterozygous	Familial	Niemeyer et al. (2010)
1	c.1210T>C	8	p.Cys404Arg	RING	Homozygous	Heterozygous	De novo	Niemeyer et al. (2010)
1	c.1222T>A	8	p.Trp408Arg	RING	Homozygous	Heterozygous	De novo	Niemeyer et al. (2010)
2	c.1228-2A>G	Intron 8	Splice-site change	RING[b]	Homozygous	NA	De novo	Niemeyer et al. (2010); Strullu et al. (2013)
1	c.1253T>C	9	p.Phe418Ser	RING	Homozygous	Heterozygous	Familial	Strullu et al. (2013)
1	c.1254C>G	9	p.Phe418Leu	RING	Homozygous	Heterozygous	Familial	Strullu et al. (2013)
1	c.1258C>G	9	p.Arg420Gly	RING/linker2	Homozygous	Heterozygous	De novo	Strullu et al. (2013)
1	c.1259G>A	9	p.Arg420Gln	RING/linker2	Heterozygous	Heterozygous	Familial	Martinelli et al. (2010)

[a]Position referred to the A of the ATG translation initiation codon in the reference cDNA sequence (NM_005188.3).
[b]Aberrant mRNA processing was demonstrated, leading to a catalytically inactive protein missing a portion of both the RING domain and the linker helix region connecting it to the TKB domain (mutations affecting intron 7), or the RING domain alone (mutation affecting intron 8).
[c]In the subject described by Hanson et al. (2014), the c.1100A>C mutation was found in an homozygous state in three independent teratoma samples. Nonhematopoietic cells were not available in two subjects carrying this lesion.
[d]This mutation occurred as a de novo event in eight subjects, whereas it was inherited in six cases.
LHR, linker helix region connecting the RING finger domain to the TKB domain; linker2, stretch connecting the RING finger domain to the proline-rich domain; NA, data not available; RING, RING finger domain; TKB, *N*-terminal tyrosine kinase-binding domain.

2009; Loh et al., 2009; Niemeyer et al., 2010]. Since RNA was not available for this patient, a minigene assay was performed to explore the consequences of the c.1096-1G>T variant on mRNA processing [Cooper, 2005]. COS1 cells were transiently transfected with the pSPL3 constructs containing either the wild-type or mutant *CBL* genomic region encompassing exon 8. Sequencing of the processed transcript RT-PCR products revealed aberrant splicing of the mutant allele, resulting in loss of the entire exon 8 (Fig. 2B and C; Supp. Fig. S2).

The c.705T>A transversion found in case 05-0562 is predicted to cause premature termination of the protein at codon 235, within the TKB domain, possibly generating a *v*-Cbl-like protein lacking E3 activity [Langdon et al., 1989; Blake et al., 1991]. RNA was not available to evaluate the extent of reduction in the level of mRNA of the transcribed mutant allele due to nonsense-mediated decay. To explore the effect of this change on protein expression and stability in vitro, and evaluate its impact on signal flow through the RAS-MAPK and PI3K-AKT cascades, we transiently expressed HA-tagged CBL^{WT}, $CBL^{Tyr235*}$, and $CBL^{Arg420Gln}$ proteins, the latter included as representative of CBL mutants acting in a dominant-negative manner [Sargin et al., 2007; Dunbar et al., 2008; Martinelli et al., 2010], in COS1 cells. Western blot analysis showed a dramatically reduced expression of the CBL Tyr^{235*} mutant compared with the wild-type protein (Fig. 3A), which was due to quick protein degradation (half-life <2 hr) as documented by cycloheximide treatment experiments (Fig. 3B). Cells expressing the $CBL^{Tyr235*}$ mutant, however, showed enhanced constitutive and EGF-induced ERK and AKT phosphorylation (Fig. 3C), suggesting a dominant-negative effect on wild-type CBL, possibly uncoupling cell-surface receptor binding to E3 ligase activity.

Clinical Features of CBL Mutation-Positive Subjects

Detailed clinical information was obtained for the five subjects harboring the germline *CBL* mutations (Supp. Table S3), and pic-

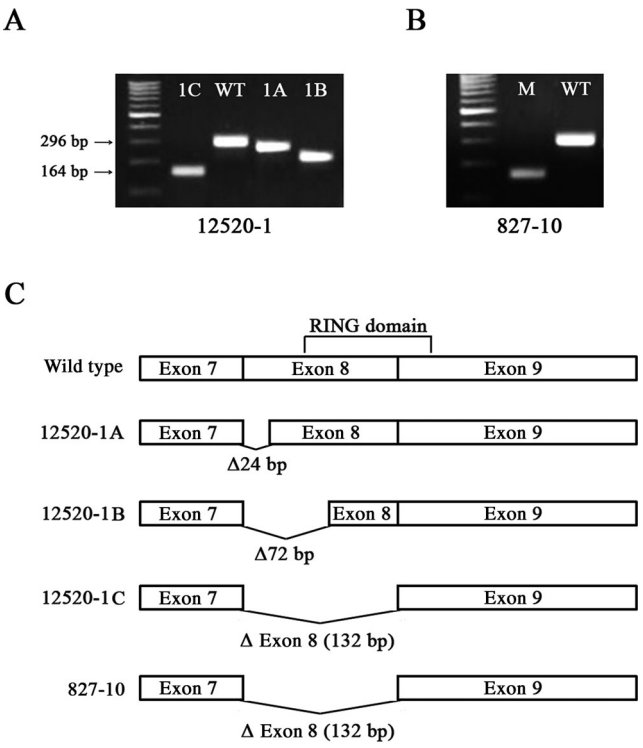

Figure 2. Consequences of the c.1096-4_1096-1delAAAG and c.1096-1G>T splice-site changes on mRNA processing. **A**: RT-PCR products obtained from cDNA of case 12520-1 (c.1096-4_1096-1delAAAG). PCR products were cloned, individual *Escherichia coli* colonies were amplified, and amplicons were separated by electrophoresis on 2% agarose gel. Wild-type (WT) amplicon (296-bp-long, lane 3) was observed in 17 out of 25 colonies, whereas the 1A (272-bp-long, lane 4), 1B (224-bp-long, lane 5), and 1C (164-bp-long, lane 2) products were identified in four, three, and one clones, respectively. **B**: Minigene assay performed to evaluate the impact of the c.1096-1G>T change (case 827-10). COS1 cells were transiently transfected with wild-type (WT) or mutant construct and lysed. cDNAs obtained from total RNA was amplified with the same primer pair used in panel **A**. Lane 1, ladder; lane 2, mutant allele (M); lane 3, WT allele. **C**: Schematic representation of the consequences of the splice-site mutations detected in patients 12520-1 and 827-10 (see Supp. Fig. S2 for chromatograms). Δ indicates deleted region.

tures were available for two of them (Fig. 1C). All patients displayed dysmorphic facial features within the RASopathy spectrum. The sporadic case heterozygous for the c.1111T>C transition was referred at 5 years because of moderate bilateral sensorineural hearing loss requiring hearing aids, mild developmental delay, and language difficulties (Wechsler Intelligence Scale for Children-Revised [WISC-R], IQ = 64, verbal = 58, performance = 74). Clinical examination at 10 years showed relative macrocephaly, short neck, mild pectus excavatum, widely spaced nipples, curly hair, dark skin, and a single café-au-lait spot on the left leg. Stature was in the normal range and cardiologic evaluation did not reveal any relevant defect. A head MRI scan showed a widened cisterna magna and cerebellar vermis hypoplasia associated with tortuosity of intracranial arteries. Despite the well-documented association between the c.1111T>C nucleotide change and JMML, this subject did not exhibit any hematologic anomaly.

The boy carrying the de novo c.1104_1112del mutation exhibited congenital left-sided cataract that had been diagnosed during the neonatal period. Echocardiography revealed mild pulmonary valve stenosis requiring no specific treatment. He was operated for inguinal hernia and undescended testis at the age of 18 months. No hematologic abnormality was ever noted. Psychomotor development was significantly delayed (walking at 30 months). At the age of 35 months, his height was 91.5 cm (10th percentile), weight was 14.1 kg (50th percentile), and head circumference was 48 cm (3rd percentile). When he was admitted for genetic re-evaluation at the age of 3 years and 2 months, he was noted to have asymmetric thorax and relatively dark skin pigmentation.

The girl heterozygous for the c.1096-4_1096-1delAAAG splice-site change had an unremarkable family history. At birth, she was hydropic and profoundly hypotonic with no respiratory effort, and required immediate resuscitation and intubation. She exhibited severe respiratory acidosis, marked bilateral pleural effusions, and chylothorax, and was found to be at grade 2 of Sarnat's hypoxic-ischemic encephalopathy scale. Her physical examination revealed diffuse cyanosis, anasarca, mild strabismus, redundant skin on the neck, shield chest with widely spaced nipples, extremities joint limitations, left hand single palmar crease, hammer toes, high arched feet, and diffuse petechiae on face and upper body. Cardiac evaluation revealed pulmonary valve stenosis and biventricular hypertrophy with severe left outflow obstruction. Neurological examination demonstrated severe hypotonia with limited spontaneous activity. Brain ultrasound showed increased white matter echogenicity and mildly underdeveloped sulci in the brain parenchyma. She also exhibited hepatosplenomegaly and bilateral hydronephrosis and hydroureters. Blood count showed persistent leukocytosis, monocytosis, and thrombocytopenia, whereas bone marrow aspirate presented elevated blast count with no evidence of chromosome rearrangements. On liver biopsy, there was prominent extramedullary hematopoiesis, supporting a diagnosis of JMML. Head circumference and linear growth decelerated quickly, settling below the 3rd percentile. At the age of 5 months, neurodevelopmental assessments demonstrated evidence of global developmental delay with poor interaction with the environment and delayed motor skills. Severely bradycardic and hypotensive, she died at the age of 6 months. Autopsy revealed diffuse edema, bilateral pulmonary effusions, extensive multifocal fibrosis, and perivascular infiltrates of nucleated erythroid and myeloid precursor cells, suggestive of extramedullary hematopoiesis.

The boy heterozygous for the c.1096-1G>T splice-site variant had a history of prenatal pleural effusions/hydrops. Clinical details had recently been reported in a separate study focused on prenatal findings associated with germline *CBL* mutations [Bülow et al., 2015]. Major postnatal features included severe feeding difficulties, failure to thrive, short stature, hypotonia, and psychomotor retardation. Splenomegaly and easy bruising without any evidence of a hematologic neoplasia persisted up to the age of 11 years, when he was last examined. Cardiac evaluation revealed mild pulmonary valve stenosis. He also showed a broad chest with mild pectus excavatum and carinatum, and hyperpigmentation of the legs. Brain MRI revealed delayed myelination, hypoplasia of the olfactory bulbs, and optic chiasm.

Finally, the boy carrying the heterozygous c.705T>A transversion was the second child of nonconsanguineous parents, appeared macrosomic (at 7 months, weight and length were at 90th and 97th percentile, respectively), but had a head circumference at the 3rd percentile. He displayed short neck with redundant skin. Developmental milestones were normal. Two-dimensional color-Doppler echocardiography revealed pulmonary valve stenosis with dysplastic pulmonary valve leaflets and poststenotic pulmonary dilation. Cerebral, renal, ophthalmological, and audiological assessments were normal. Clinical evaluation of the affected mother (35-year old) and brother (4.3-year old) documented high forehead, downslanting palpebral fissures, thick lips, low-set, and dysmorphic ears with

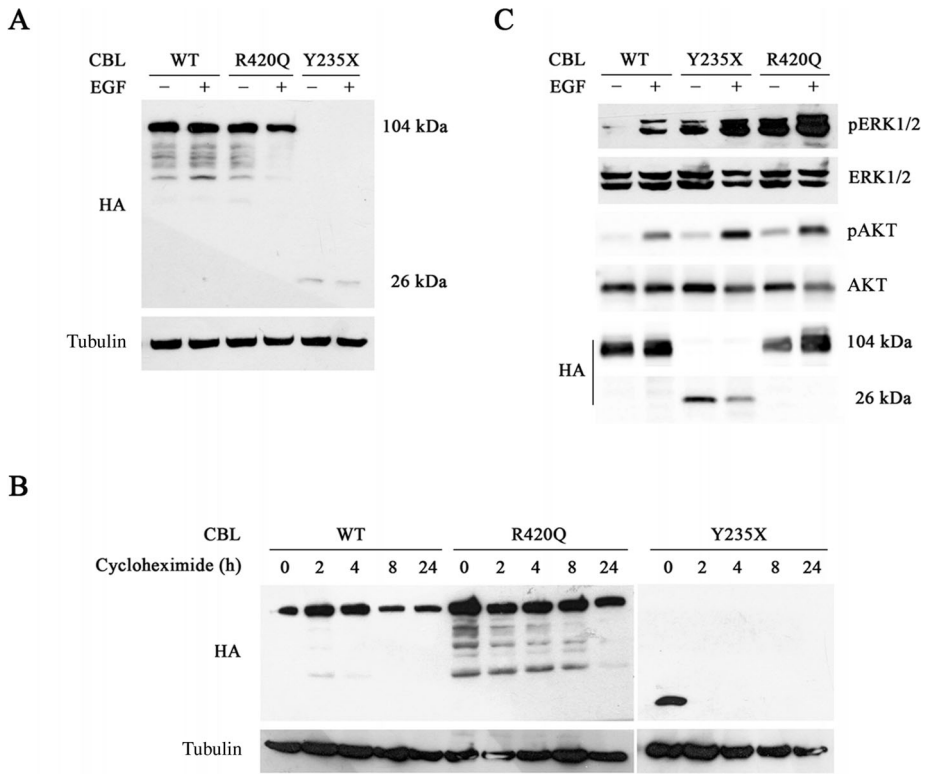

Figure 3. Functional characterization of the CBL^{Tyr235*} mutant. **A**: Expression levels of exogenous CBL in COS1 cells transiently expressing wild-type CBL, and the CBL^{Arg420Gln} and CBL^{Tyr235*} mutants. Whole cell extracts were probed with anti-HA and anti-β-tubulin antibodies. **B**: Time course analysis of CBL stability after cycloheximide treatment. Twenty-four hours following transfection, COS1 cells were treated with cycloheximide at 100 μg/ml to prevent protein synthesis, at the indicated times, and probed with anti-HA and anti-β-tubulin antibodies. Blot with the truncated mutant (right panel) was exposed four times longer than that displaying the wild-type and p.Arg420Gln proteins (left panel) to appreciate the expression levels of the former. **C**: Determination of ERK and AKT phosphorylation levels in transiently transfected COS1 cells. Protein phosphorylation status (pERK1/2 and pAKT) was evaluated basally or following EGF stimulation (100 ng/ml, 30 min). Total ERK and AKT levels in cell lysates are shown for equal protein expression and loading. Representative blots of three performed experiments are shown.

thick helices, and low-posterior hairlines. The proband's brother also showed a flat nasal bridge, palpebral ptosis, hyperkeratosis, and short neck. Both individuals, however, had normal stature and did not display any cardiac defect.

Clinical Spectrum of CBL Mutations and Genotype–Phenotype Correlation Analyses

A review of the literature allowed us to collect extensive clinical data for 13 subjects carrying germline *CBL* mutations, whereas incomplete information was available for 18 additional individuals originally studied on the basis of JMML/AML occurrence (Supp. Table S3). Overall, analysis of the available clinical records confirmed previous observations from our group and others indicating that *CBL* mutations are associated with a variable phenotype resembling, in part, NS, and confer predisposition to JMML. Notably, while a particularly severe phenotype was observed in a small subset of patients, clinical features appeared quite subtle in the majority of cases. We noticed a lower prevalence of individuals exhibiting reduced growth (stature below the 3rd percentile) (11/36 vs. 84/115, $P < 0.0001$, Fisher's exact test), cryptorchidism (5/18 vs. 64/83, $P < 0.0002$), and cardiac defects (12/36 vs. 132/151, $P < 0.0001$), compared with what observed in the NS general population [Sarkozy et al., 2009]. Pulmonary valve stenosis and HCM were detected in 17% ($P < 0.0001$) and 8% of cases, respectively. Craniofacial features were always present but generally mild. Ectodermal and skeletal involvement was frequently observed, with thin/sparse hair, café-au-lait spots, and thorax anomalies being the most recurrent features. Five out of 17 cases reported by Niemeyer et al. (2010) and one additional patient [Strullu et al., 2013] exhibited juvenile xanthogranuloma. Interestingly, *CBL* mutation-positive subjects displayed a relatively high frequency of neurological features, including psychomotor delay (65%), cognitive delay (35%), and muscular hypotonia (50%). Head MRI documented delayed myelination, abnormal corpus callosum, and cerebellar vermis hypoplasia in two unrelated individuals, whereas Arnold–Chiari malformation type I, mild left cerebral atrophy, widened cisterna magna, and moyamoya disease were reported in one patient each. Recurrent complications also included ocular anomalies (22%) and hearing loss (17%).

Discussion

CBL is a widely expressed E3 ubiquitin ligase that negatively regulates intracellular signaling downstream of RTKs [Swaminathan and Tsygankov, 2006; Dikic and Schmidt, 2007]. Germline *CBL* mutations have been established to cause a previously unrecognized RASopathy with variable phenotype [Martinelli et al., 2010; Niemeyer et al., 2010; Pérez et al., 2010]. In this work, we provided new data on the molecular spectrum of germline *CBL* mutations

and more comprehensively assessed the clinical features associated with *CBL* lesions.

Since the discovery of *CBL* as a RASopathy gene, 44 germline *CBL* mutations have been identified. Combined data indicate that these lesions are predominantly missense changes (82.4%; 95% CI, 69.6%–95.2%) affecting residues located within the RING finger domain or the LHR. Among those lesions, approximately 50% involves Tyr^{371}, with the p.Tyr371His amino acid substitution being the most recurrent change. Tyr^{371} plays a crucial role in the activation of CBL E3 ligase activity [Dou et al., 2012]. The available crystal structure data are consistent with a model of CBL functional regulation in which, in the absence of the substrate, the enzyme adopts an autoinhibited conformation with the TKB domain binding to the RING finger domain and masking the E2-binding sites. Following Tyr^{371} phosphorylation, the LHR undergoes a conformational change that abrogates autoinhibition and brings the RING domain and E2 nearby the substrate-binding site, thus promoting E3 activity. Extensive studies demonstrated that E3 activation is required for RTKs ubiquitination [Levkowitz et al., 1999; Thien et al., 2001; Sanada et al., 2009; Niemeyer et al., 2010]. Consistent with that, mutations affecting Tyr^{371} was shown to abrogate the ability of CBL to ubiquitinate FLT3, KIT, and EGFR [Sanada et al., 2009; Niemeyer et al., 2010].

Heterozygous variants affecting splicing of *CBL* have been observed in a significant fraction of cases (11.8%; 95% CI, 0.9%–22.6%), the majority resulting in loss of the sequence encoding amino acid stretched encompassing Tyr^{371}. In the present cohort, case 12520-1 carrying the c.1096-4_1096-1delAAAG mutation, which disrupts the splice acceptor site for exon 8, exhibited a severe RASopathy phenotype with JMML. Interestingly, we failed to identify loss of the wild-type allele in leukemic cells from this subject. This finding mirrored available data indicating that somatically acquired *CBL* deletions arising from aberrant splicing are frequently heterozygous, whereas the vast majority of missense mutations are homozygous as a consequence of 11q isodisomy [Kales et al., 2010; Strullu et al., 2013]. In line with this evidence, the splice-site mutations detected in MOLM-13 and MOLM-14 cell lines and NUP98-HOXD13 transgenic mice were also heterozygous [Caligiuri et al., 2007; Abbas et al., 2008; Slape et al., 2008; Reindl et al., 2009]. These findings suggest that in-frame deletions of the LHR/RING domains of CBL might confer stronger transforming properties than missense mutations. Further studies are required to test this hypothesis.

One small in-frame indel and a nonsense mutation occurring in two patients were also identified. While the former, leading to deletion of three highly conserved residues including Tyr^{371}, had previously been described in leukemia [Sanada et al., 2009], the latter is a novel change causing premature termination of the protein at residue 235, within the calcium-binding EF hand of the TKB domain. This motif plays a key role in maintaining the TKB structure, allowing proper binding of the ligase to protein tyrosine kinases [Lupher et al., 1999; Meng et al., 1999]. Truncating mutations affecting the TKB domain of CBL rarely occur as somatic events in cancer (COSMIC database, http://cancer.sanger.ac.uk/cancergenome/projects/cosmic/). In particular, heterozygous nonsense mutations at codons Gln^{175} and Arg^{343} were observed in a lung carcinoma sample and a CMML subject carrying a concomitant p.Cys384Tyr amino acid change, respectively [Sanada et al., 2009; Imielinski et al., 2012]. These transcripts coding for truncated proteins are expected to be recognized and degraded via nonsense-mediated mRNA decay (NMD), an evolutionary conserved mechanism used by eukaryotes to prevent the production of aberrant proteins with deleterious gain-of-function or dominant-negative effects [Frischmeyer and Dietz, 1999], suggesting haploinsufficiency as the underlying molecular mechanism. Accumulating data, however, document high variability in NMD efficiency [Miller and Pearce, 2014], suggesting that a consistent fraction of these nonsense transcripts might generate *v*-Cbl-like proteins with dominant-negative function. *v*-Cbl, the transforming gene of the Cas NS-1 retrovirus, is a truncated 357 residue-long CBL protein able to induce B-cell lymphomas and myeloid leukemia in mice [Langdon et al., 1989; Blake et al., 1991]. This protein functions in a dominant-negative manner by uncoupling CBL binding to activated RTKs from their ubiquitination and degradation. Consistently, our in vitro functional data documented enhanced ERK and AKT phosphorylation in cells expressing the p.Tyr235* mutant.

Extensive studies demonstrate that germline-transmitted and somatically acquired mutations in RASopathy genes rarely overlap [Tartaglia et al., 2011], *PTPN11* being the archetypal example [Tartaglia et al., 2006]. In that case, NS-causing mutations confer milder gain-of-function effects than the cancer-associated lesions do, with the former being sufficient to perturb biological processes that are strictly controlled by SHP2, but inadequate to deregulate significantly processes that are less strictly controlled by the phosphatase. Similarly, mutations in *NRAS*, *KRAS*, and *BRAF* underlying NS and cardiofaciocutaneous syndrome (CFCS; MIM #115150), as well as those involving *HRAS* in Costello syndrome (CS; MIM #218040), rarely occur as oncogenic defects [Aoki et al., 2008; Tartaglia et al., 2011]. Conversely, the molecular spectra of germline and somatic *CBL* mutations largely overlap, suggesting that these lesions have generally milder consequences on development than cancer-associated mutations in most RASopathy genes. Of note, however, missense mutations involving Tyr^{371} have been identified rarely in subjects with *CBL* mutation-associated syndrome without JMML (~10% of cases), whereas they represent the most common lesions among individuals with *CBL* mutation-positive syndromic JMML (~50% of cases). This observation indicates that patients carrying a germline defect altering codon 371 are at risk for developing JMML. Consistent with this, codon 371 represents a "hot spot" for somatic *CBL* mutations in isolated JMML, whereas it is rarely mutated in acute leukemias [Kales et al., 2010].

The present study is in line with our previous estimate of *CBL* mutation prevalence, indicating that defects in this gene account for <1% of subjects with clinical features resembling NS, even though they might be more common among individuals with features within the RASopathy phenotypic spectrum. Although the clinical spectrum associated with *CBL* mutations is wide, genotype–phenotype correlations seem to exist. Specifically, *CBL* mutation-positive patients exhibit a relatively lower prevalence of cardiac defects (33%) compared with the general NS population, for which an estimate of up to 80% has been reported [Burch et al., 1993; Marino et al., 1999; Shaw et al., 2007; Sarkozy et al., 2009]. Of note, CHDs were observed in all subjects carrying the p.Glu367Pro amino acid change ($N = 4$), whereas only one out of 12 patients with a missense mutation at codon 371, for which clinical data were available, had a cardiac defect (HCM). Short stature is a common feature in NS, although adult height is not always adversely affected. Clinical data revealed that length/stature is less frequently below the 3rd percentile (31%) in cases with mutated *CBL* compared with *PTPN11* mutation-positive NS subjects (93%) [Roberts et al., 2013], similar to what reported in individuals with *SOS1* mutations [Tartaglia et al., 2007; Lepri et al., 2011]. Finally, *CBL* mutation-positive patients displayed a high frequency of head MRI findings associated or not with structural brain abnormalities (54%), which are usually rare in NS, but more frequently occur in other RASopathies, such as CFCS [Roberts et al., 2006]. Among these, case 827-10 showed delayed brain myelination, a feature that

was observed in one subject from our previous cohort [Martinelli et al., 2010]. Similar anomalies represent a relatively common feature in CFCS patients with a *BRAF* mutation [Yoon et al., 2007; Aizaki et al., 2011]. Of note, conditional ablation of *Braf* in mouse neuroglial precursor cells was shown to result in defective myelination and oligodendrocyte differentiation [Galabova-Kovacs et al., 2008]. Similarly, loss of Shp2 in the oligodendrocyte lineage, as well as transgenic expression of a NS-associated Shp2 gain-of-function allele, results in severe abnormal myelination phenotypes [Ehrman et al., 2014]. Hence, the myelination defect observed in some individuals with a *CBL* mutation adds support to the impact of dysregulated RAS signaling on glial cell development. Of note, patient 10-0746 and case HD316 from our previous cohort [Martinelli et al., 2010] showed cerebellar vermis hypoplasia, an unreported feature in RASopathies. Besides these atypical findings, additional brain anomalies (e.g., Arnold–Chiari malformation type I, hypoplastic corpus callosum, mild brain atrophy, and cerebrovascular defects) occur more frequently in NS and related disorders [Schon et al., 1992; Ganesan and Kirkham, 1997; Galarza et al., 2010; Aizaki et al., 2011; Keh et al., 2013; Okamoto et al., 2014].

Overall, the present analysis indicates that patients heterozygous for a germline *CBL* mutation exhibit a wide phenotypic variability partially overlapping NS. Besides the occurrence of a subtle phenotype in a large proportion of subjects, clinical features are particularly severe in a small number of cases. Although available data suggest possible genotype–phenotype correlations, based on the increasing evidence documenting co-occurrence of mutations in functionally related genes [Nystrom et al., 2009; Tang et al., 2009; Thiel et al., 2009; Longoni et al., 2010], the possibility that lesions concomitant to those involving *CBL* might modulate the phenotype in some of these individuals cannot be ruled out. Analysis of the phenotypic spectrum associated with *CBL* mutations indicates that molecular scanning of this gene would be worthwhile in patients with facial features resembling NS associated with brain anomalies, but normal cardiac development and growth, as well as in subjects with NS/JMML without mutations in known disease genes.

Acknowledgments

We are indebted to the patients and families who participated in the study, and the physicians who referred the subjects. We thank Serenella Venanzi (Istituto Superiore di Sanità, Rome, Italy) and Angela Alberico (Laboratorio Mendel, Istituto di Ricovero e Cura a Carattere Scientifico-Casa Sollievo della Sofferenza, Rome, Italy) for technical assistance.

Disclosure statement: The authors declare no conflict of interest.

References

Abbas S, Rotmans G, Löwenberg B, Valk PJ. 2008. Exon 8 splice site mutations in the gene encoding the E3-ligase CBL are associated with core binding factor acute myeloid leukemias. Haematologica 93:1595–1597.

Aizaki K, Sugai K, Saito Y, Nakagawa E, Sasaki M, Aoki Y, Matsubara Y. 2011. Cardiofacio-cutaneous syndrome with infantile spasms and delayed myelination. Brain Dev 33:166–169.

Allanson JE. 2007. Noonan syndrome. Am J Med Genet C Semin Med Genet 145C:274–279.

Aoki Y, Matsubara Y. 2013. Ras/MAPK syndromes and childhood hemato-oncological diseases. Int J Hematol 97:30–36.

Aoki Y, Niihori T, Banjo T, Okamoto N, Mizuno S, Kurosawa K, Ogata T, Takada F, Yano M, Ando T, Hoshika T, Barnett C, et al. 2013. Gain-of-function mutations in RIT1 cause Noonan syndrome, a RAS/MAPK pathway syndrome. Am J Hum Genet 93:173–180.

Aoki Y, Niihori T, Narumi Y, Kure S, Matsubara Y. 2008. The RAS/MAPK syndromes: novel roles of the RAS pathway in human genetic disorders. Hum Mutat 29:992–1006.

Becker H, Yoshida K, Blagitko-Dorfs N, Claus R, Pantic M, Abdelkarim M, Niemöller C, Greil C, Hackanson B, Shiraishi Y, Chiba K, Tanaka H, et al. 2014. Tracing the development of acute myeloid leukemia in CBL mutation-associated syndrome. Blood 123:1883–1886.

Blake TJ, Shapiro M, Morse HC 3rd, Langdon WY. 1991. The sequences of the human and mouse c-cbl proto-oncogenes show v-cbl was generated by a large truncation encompassing a proline-rich domain and a leucine zipper-like motif. Oncogene 6:653–657.

Brand K, Kentsch H, Glashoff C, Rosenberger G. 2014. RASopathy-associated CBL germline mutations cause aberrant ubiquitylation and trafficking of EGFR. Hum Mutat 35:1372–1381.

Bülow L, Lissewski C, Bressel R, Rauch A, Stark Z, Zenker M, Bartsch O. 2015. Hydrops, fetal pleural effusions and chylothorax in three patients with CBL mutations. Am J Med Genet A 167A:394–399.

Burch M, Sharland M, Shinebourne E, Smith G, Patton M, McKenna W. 1993. Cardiologic abnormalities in Noonan syndrome: phenotypic diagnosis and echocardiographic assessment of 118 patients. J Am Coll Cardiol 22:1189–1192.

Caligiuri MA, Briesewitz R, Yu J, Wang L, Wei M, Arnoczky KJ, Marburger TB, Wen J, Perrotti D, Bloomfield CD, Whitman SP. 2007. Novel c-CBL and CBL-b ubiquitin ligase mutations in human acute myeloid leukemia. Blood 110:1022–1024.

Cooper TA. 2005. Use of minigene systems to dissect alternative splicing elements. Methods 37:331–340.

Dikic I, Schmidt MH. 2007. Malfunctions within the Cbl interactome uncouple receptor tyrosine kinases from destructive transport. Eur J Cell Biol 86:505–512.

Dou H, Buetow L, Hock A, Sibbet GJ, Vousden KH, Huang DT. 2012. Structural basis for autoinhibition and phosphorylation-dependent activation of c-Cbl. Nat Struct Mol Biol 19:184–192.

Dunbar AJ, Gondek LP, O'Keefe CL, Makishima H, Rataul MS, Szpurka H, Sekeres MA, Wang XF, McDevitt MA, Maciejewski JP. 2008. 250K single nucleotide polymorphism array karyotyping identifies acquired uniparental disomy and homozygous mutations, including novel missense substitutions of c-Cbl, in myeloid malignancies. Cancer Res 68:10349–10357.

Ehrman LA, Nardini D, Ehrman S, Rizvi TA, Gulick J, Krenz M, Dasgupta B, Robbins J, Ratner N, Nakafuku M, Waclaw RR. 2014. The protein tyrosine phosphatase Shp2 is required for the generation of oligodendrocyte progenitor cells and myelination in the mouse telencephalon. J Neurosci 34:3767–3778.

Flex E, Jaiswal M, Pantaleoni F, Martinelli S, Strullu M, Fansa EK, Caye A, De Luca A, Lepri F, Dvorsky R, Pannone L, Paolacci S, et al. 2014. Activating mutations in RRAS underlie a phenotype within the RASopathy spectrum and contribute to leukaemogenesis. Hum Mol Genet 23:4315–4327.

Frischmeyer PA, Dietz HC. 1999. Nonsense-mediated mRNA decay in health and disease. Hum Mol Genet 8:1893–1900.

Galabova-Kovacs G, Catalanotti F, Matzen D, Reyes GX, Zezula J, Herbst R, Silva A, Walter I, Baccarini M. 2008. Essential role of B-Raf in oligodendrocyte maturation and myelination during postnatal central nervous system development. J Cell Biol 180:947–955.

Galarza M, Martínez-Lage JF, Ham S, Sood S. 2010. Cerebral anomalies and Chiari type 1 malformation. Pediatr Neurosurg 46:442–449.

Ganesan V, Kirkham FJ. 1997. Noonan syndrome and moyamoya. Pediatr Neurol 16:256–258.

Grand FH, Hidalgo-Curtis CE, Ernst T, Zoi K, Zoi C, McGuire C, Kreil S, Jones A, Score J, Metzgeroth G, Oscier D, Hall A, et al. 2009. Frequent CBL mutations associated with 11q acquired uniparental disomy in myeloproliferative neoplasms. Blood 113:6182–6192.

Hanson HL, Wilson MJ, Short JP, Chioza BA, Crosby AH, Nash RM, Marks KJ, Mansour S. 2014. Germline CBL mutation associated with a noonan-like syndrome with primary lymphedema and teratoma associated with acquired uniparental isodisomy of chromosome 11q23. Am J Med Genet A 164A:1003–1009.

Hyakuna N, Muramatsu H, Higa T, Chinen Y, Wang X, Kojima S. 2015. Germline mutation of CBL is associated with moyamoya disease in a child with juvenile myelomonocytic leukemia and Noonan syndrome-like disorder. Pediatr Blood Cancer 62:542–544.

Imielinski M, Berger AH, Hammerman PS, Hernandez B, Pugh TJ, Hodis E, Cho J, Suh J, Capelletti M, Sivachenko A, Sougnez C, Auclair D, et al. 2012. Mapping the hallmarks of lung adenocarcinoma with massively parallel sequencing. Cell 150:1107–1120.

Jongmans MC, van der Burgt I, Hoogerbrugge PM, Noordam K, Yntema HG, Nillesen WM, Kuiper RP, Ligtenberg MJ, van Kessel AG, van Krieken JH, Kiemeney LA, Hoogerbrugge N. 2011. Cancer risk in patients with Noonan syndrome carrying a PTPN11 mutation. Eur J Hum Genet 19:870–874.

Kales SC, Ryan PE, Nau MM, Lipkowitz S. 2010. Cbl and human myeloid neoplasms: the Cbl oncogene comes of age. Cancer Res 70:4789–4794.

Kassenbrock CK, Anderson SM. 2004. Regulation of ubiquitin protein ligase activity in c-Cbl by phosphorylation-induced conformational change and constitutive activation by tyrosine to glutamate point mutations. J Biol Chem 279:28017–28027.

Keh YS, Abernethy L, Pettorini B. 2013. Association between Noonan syndrome and Chiari I malformation: a case-based update. Childs Nerv Syst 29:749–752.

Kratz CP, Rapisuwon S, Reed H, Hasle H, Rosenberg PS. 2011. Cancer in Noonan, Costello, cardiofaciocutaneous and LEOPARD syndromes. Am J Med Genet C Semin Med Genet 157C:83–89.

Langdon WY, Hartley JW, Klinken SP, Ruscetti SK, Morse HC 3rd. 1989. v-cbl, an oncogene from a dual-recombinant murine retrovirus that induces early B-lineage lymphomas. Proc Natl Acad Sci USA 86:1168–1172.

Lepri F, De Luca A, Stella L, Rossi C, Baldassarre G, Pantaleoni F, Cordeddu V, Williams BJ, Dentici ML, Caputo V, Venanzi S, Bonaguro M, et al. 2011. SOS1 mutations in Noonan syndrome: molecular spectrum, structural insights on pathogenic effects, and genotype-phenotype correlations. Hum Mutat 32:760–772.

Levkowitz G, Waterman H, Ettenberg SA, Katz M, Tsygankov AY, Alroy I, Lavi S, Iwai K, Reiss Y, Ciechanover A, Lipkowitz S, Yarden Y. 1999. Ubiquitin ligase activity and tyrosine phosphorylation underlie suppression of growth factor signaling by c-Cbl/Sli-1. Mol Cell 4:1029–1040.

Loh ML, Sakai DS, Flotho C, Kang M, Fliegauf M, Archambeault S, Mullighan CG, Chen L, Bergstraesser E, Bueso-Ramos CE, Emanuel PD, Hasle H, et al. 2009. Mutations in CBL occur frequently in juvenile myelomonocytic leukemia. Blood 114:1859–1863.

Longoni M, Moncini S, Cisternino M, Morella IM, Ferraiuolo S, Russo S, Mannarino S, Brazzelli V, Coi P, Zippel R, Venturin M, Riva P. 2010. Noonan syndrome associated with both a new Jnk-activating familial SOS1 and a de novo RAF1 mutations. Am J Med Genet A 152A:2176–2184.

Lupher ML Jr, Rao N, Eck MJ, Band H. 1999. The Cbl protooncoprotein: a negative regulator of immune receptor signal transduction. Immunol Today 20:375–382.

Marino B, Digilio MC, Toscano A, Giannotti A, Dallapiccola B. 1999. Congenital heart diseases in children with Noonan syndrome: an expanded cardiac spectrum with high prevalence of atrioventricular canal. J Pediatr 135:703–706.

Martinelli S, De Luca A, Stellacci E, Rossi C, Checquolo S, Lepri F, Caputo V, Silvano M, Buscherini F, Consoli F, Ferrara G, Digilio MC, et al. 2010. Heterozygous germline mutations in the CBL tumor-suppressor gene cause a Noonan syndrome-like phenotype. Am J Hum Genet 87:250–257.

Martinelli S, Checquolo S, Consoli F, Stellacci E, Rossi C, Silvano M, Franciosa G, Flex E, Cossu C, De Luca A, Foà R, Cazzaniga G, et al. 2012. Loss of CBL E3-ligase activity in B-lineage childhood acute lymphoblastic leukaemia. Br J Haematol 159:115–119.

Mendez HM, Opitz JM. 1985. Noonan syndrome: a review. Am J Med Genet 21:493–506.

Meng W, Sawasdikosol S, Burakoff SJ, Eck MJ. 1999. Structure of the amino-terminal domain of Cbl complexed to its binding site on ZAP-70 kinase. Nature 398:84–90.

Miller JN, Pearce DA. 2014. Nonsense-mediated decay in genetic disease: friend or foe? Mutat Res Rev Mutat Res 762C:52–64.

Muramatsu H, Makishima H, Jankowska AM, Cazzolli H, O'Keefe C, Yoshida N, Xu Y, Nishio N, Hama A, Yagasaki H, Takahashi Y, Kato K, et al. 2010. Mutations of an E3 ubiquitin ligase c-Cbl but not TET2 mutations are pathogenic in juvenile myelomonocytic leukemia. Blood 115:1969–1975.

Neel BG, Gu H, Pao L. 2003. The 'Shp'ing news: SH2 domain-containing tyrosine phosphatases in cell signaling. Trends Biochem Sci 28:284–293.

Niemeyer CM, Kang MW, Shin DH, Furlan I, Erlacher M, Bunin NJ, Bunda S, Finklestein JZ, Sakamoto KM, Gorr TA, Mehta P, Schmid I, et al. 2010. Germline CBL mutations cause developmental abnormalities and predispose to juvenile myelomonocytic leukemia. Nat Genet 42:794–800.

Nystrom AM, Ekvall S, Strömberg B, Holmström G, Thuresson AC, Annerén G, Bondeson ML. 2009. A severe form of Noonan syndrome and autosomal dominant café-au-lait spots-evidence for different genetic origins. Acta Paediatr 98:693–698.

Okamoto N, Miya F, Tsunoda T, Kato M, Saitoh S, Yamasaki M, Shimizu A, Torii C, Kanemura Y, Kosaki K. 2014. Targeted next-generation sequencing in the diagnosis of neurodevelopmental disorders. Clin Genet. [Epub ahead of print]

Pérez B, Mechinaud F, Galambrun C, Ben Romdhane N, Isidor B, Philip N, Derain-Court J, Cassinat B, Lachenaud J, Kaltenbach S, Salmon A, Désirée C, et al. 2010. Germline mutations of the CBL gene define a new genetic syndrome with predisposition to juvenile myelomonocytic leukaemia. J Med Genet 47:686–691.

Rauen KA. 2013. The RASopathies. Annu Rev Genomics Hum Genet 14:355–369.

Reindl C, Quentmeier H, Petropoulos K, Greif PA, Benthaus T, Argiropoulos B, Mellert G, Vempati S, Duyster J, Buske C, Bohlander SK, Humphries KR, et al. 2009. CBL exon 8/9 mutants activate the FLT3 pathway and cluster in core binding factor/11q deletion acute myeloid leukemia/myelodysplastic syndrome subtypes. Clin Cancer Res 15:2238–2247.

Roberts A, Allanson J, Jadico SK, Kavamura MI, Noonan J, Opitz JM, Young T, Neri G. 2006. The cardiofaciocutaneous syndrome. J Med Genet 43:833–842.

Roberts AE, Allanson JE, Tartaglia M, Gelb BD. 2013. Noonan syndrome. Lancet 381:333–342.

Sanada M, Suzuki T, Shih LY, Otsu M, Kato M, Yamazaki S, Tamura A, Honda H, Sakata-Yanagimoto M, Kumano K, Oda H, Yamagata T, et al. 2009. Gain-of-function of mutated C-CBL tumour suppressor in myeloid neoplasms. Nature 460:904–908.

Sargin B, Choudhary C, Crosetto N, Schmidt MH, Grundler R, Rensinghoff M, Thiessen C, Tickenbrock L, Schwäble J, Brandts C, August B, Koschmieder S, et al. 2007. Flt3-dependent transformation by inactivating c-Cbl mutations in AML. Blood 110:1004–1012.

Sarkozy A, Digilio MC, Marino B, Dallapiccola B. 2009. Genotype-phenotype correlations in Noonan syndrome. In: Zenker M, editor. *Monographs human genetic noonan syndrome and related disorders*, Vol 17. Basel, Switzerland: Karger. p 40–54.

Schon F, Bowler J, Baraitser M. 1992. Cerebral arteriovenous malformation in Noonan's syndrome. Postgrad Med J 68:37–40.

Slape C, Liu LY, Beachy S, Aplan PD. 2008. Leukemic transformation in mice expressing a NUP98-HOXD13 transgene is accompanied by spontaneous mutations in Nras, Kras, and Cbl. Blood 112:2017–2019.

Shaw AC, Kalidas K, Crosby AH, Jeffery S, Patton MA. 2007. The natural history of Noonan syndrome: a long-term follow-up study. Arch Dis Child 92:128–132.

Strullu M, Caye A, Cassinat B, Fenneteau O, Touzot F, Blauwblomme T, Rodriguez R, Latour S, Petit A, Barlogis V, Galambrun C, Leblanc T, et al. 2013. In hematopoietic cells with a germline mutation of CBL, loss of heterozygosity is not a signature of juvenile myelo-monocytic leukemia. Leukemia 27:2404–2407.

Swaminathan G, Tsygankov AY. 2006. The Cbl family proteins: ring leaders in regulation of cell signaling. J Cell Physiol 209:21–43.

Tang S, Hoshida H, Kamisago M, Yagi H, Momma K, Matsuoka R. 2009. Phenotype-genotype correlation in a patient with co-occurrence of Marfan and LEOPARD syndromes. Am J Med Genet A 149A:2216–2219.

Tartaglia M, Gelb BD. 2010. Disorders of dysregulated signal traffic through the RAS-MAPK pathway: phenotypic spectrum and molecular mechanisms. Ann NY Acad Sci 1214:99–121.

Tartaglia M, Gelb BD, Zenker M. 2011. Noonan syndrome and clinically related disorders. Best Pract Res Clin Endocrinol Metab 25:161–179.

Tartaglia M, Kalidas K, Shaw A, Song X, Musat DL, van der Burgt I, Brunner HG, Bertola D, Crosby A, Ion A, Kucherlapati RS, Jeffery S, et al. 2002. PTPN11 Mutations in Noonan Syndrome: Molecular Spectrum, Genotype-Phenotype Correlation, and Phenotypic Heterogeneity. Am J Hum Genet 70:1555–1563.

Tartaglia M, Martinelli S, Stella L, Bocchinfuso G, Flex E, Cordeddu V, Zampino G, Burgt I, Palleschi A, Petrucci TC, Sorcini M, Schoch C, et al. 2006. Diversity and functional consequences of germline and somatic PTPN11 mutations in human disease. Am J Hum Genet 78:279–290.

Tartaglia M, Mehler EL, Goldberg R, Zampino G, Brunner HG, Kremer H, van der Burgt I, Crosby AH, Ion A, Jeffery S, Kalidas K, Patton MA, et al. 2001. Mutations in PTPN11, encoding the protein tyrosine phosphatase SHP-2, cause Noonan syndrome. Nat Genet 29:465–468.

Tartaglia M, Niemeyer CM, Fragale A, Song X, Buechner J, Jung A, Hählen K, Hasle H, Licht JD, Gelb BD. 2003. Somatic mutations in PTPN11 in juvenile myelomonocytic leukemia, myelodysplastic syndromes and acute myeloid leukemia. Nat Genet 34:148–150.

Tartaglia M, Pennacchio LA, Zhao C, Yadav KK, Fodale V, Sarkozy A, Pandit B, Oishi K, Martinelli S, Schackwitz W, Ustaszewska A, Martin J, et al. 2007. Gain-of-function SOS1 mutations cause a distinctive form of Noonan syndrome. Nat Genet 39:75–79.

Thiel C, Wilken M, Zenker M, Sticht H, Fahsold R, Gusek-Schneider GC, Rauch A. 2009. Independent NF1 and PTPN11 mutations in a family with neurofibromatosis-Noonan syndrome. Am J Med Genet A 149A:1263–1267.

Thien CB, Walker F, Langdon WY. 2001. RING finger mutations that abolish c-Cbl-directed polyubiquitination and downregulation of the EGF receptor are insufficient for cell transformation. Mol Cell 7:355–365.

van der Burgt I. 2007. Noonan syndrome. Orphanet J Rare Dis 2:4.

Yoon G, Rosenberg J, Blaser S, Rauen KA. 2007. Neurological complications of cardio-facio-cutaneous syndrome. Dev Med Child Neurol 49:894–899.